



RESEARCH ARTICLE

EFFECT OF PRE-HANDLING AND POST-TREATMENT CONDITIONS IN THE DEVELOPMENT OF GREEN POLYPROPYLENE COMPOSITE SLAB

Md Fauzan Kamal Mohd Yapandi^{1,2,*}, Famiza Abdul Latif¹, Mohammad Noor Jalil¹, Nurul Dhabitah Basri¹, Sharil Fadli Mohamad Zamri¹, Nabilah Akemal Muhd Zailani³, Noor Najmi Bonnia¹

¹*Faculty of Applied Sciences, University Teknologi MARA, 40450 Shah Alam, Selangor, Malaysia.*

²*TNB Research Sdn. Bhd., No. 1, Kawasan Institusi Penyelidikan, Jalan Ayer Itam, 43000 Kajang, Selangor, Malaysia.*

³*Universiti Teknologi MARA Cawangan Perlis, Kampus Arau, 02600 Arau, Perlis.*

Abstract. Electricity generation in Malaysia produces large volumes of coal bottom ash (CBA), which often accumulates in ash ponds or landfills, posing environmental risks. This study examines the potential of using CBA as a reinforcing filler in polypropylene (PP) composites to develop a sustainable and environmentally friendly material. The impact of pre-treatment (sieving) and post-treatment (heat exposure) on the physical and mechanical attributes of PP-CBA composite slabs was thoroughly examined. Findings revealed that filtering the CBA to a uniform particle size (~250 μm) significantly enhanced composite consistency, resulting in improved polymer-filler interaction, better bonding, and overall structural stability. However, subjecting the slabs to heat at 50 °C and 100 °C created a more porous structure due to moisture loss, which negatively affected crystallinity, durability, and mechanical resilience. Fourier-transform infrared spectroscopy (FTIR) and X-ray diffraction (XRD) results indicated a reduction in Silanol (Si-OH) groups and isotactic polypropylene (i-PP) peaks, confirming a decrease in crystallinity. The drop impact tests indicated that heated slabs exhibited reduced impact strength compared to untreated ones, with impact values decreasing from 3.4 J (sieved CBA) to 2.1 J (un-sieved CBA), further declining in heat-treated samples. The increase in impact strength observed with sieved CBA suggests that uniform particle distribution enhances mechanical integrity, making it a suitable candidate for applications in construction materials, lightweight structural panels, utility protection slabs, automotive components and furniture. However, moisture management and processing optimization are critical for maintaining mechanical performance and durability. Overall, this study supports the utilization of CBA into value-added materials, aligning with sustainable development and circular economy goals.

Keywords: Coal bottom ash, polymer composite, green composite, polypropylene composite.

Article Info

Received 25 February 2025

Accepted 27 February 2025

Published 2 June 2025

***Corresponding author: fauzankamal@tnb.com.my**

Copyright Malaysian Journal of Microscopy (2025). All rights reserved.

ISSN: 1823-7010, eISSN: 2600-7444

1. INTRODUCTION

In Peninsular Malaysia, coal remains a key energy source supporting the rising electricity demand [1]. The combustion of coal generates by-products such as coal fly ash (CFA), which accounts for over 80%, and coal bottom ash (CBA), making up more than 20% [2]. By 2030, electricity consumption is anticipated to reach 7,571 kWh per capita, more than double from 2002, driven by intense industrial and residential demands as Malaysia becomes an industrialized nation [3]. As Malaysia's electricity demand continues to rise, coal power plants annually consume approximately 1.5 million tons of coal [4]. These coal combustion by-products contain hazardous elements, including arsenic, cadmium, cobalt, chromium, manganese, nickel, lead, and zinc, which pose potential health and environmental threats [5]. The accumulation of CBA in landfills [6] has raised concerns due to its porous granular structure, limiting its potential applications [7]. In some cases, CBA waste has been discarded into water bodies, such as ponds, lagoons, or the ocean, in slurry form [8]. This disposal method can lead to heavy metal leaching under acidic conditions, contaminating soil, surface water, and groundwater, ultimately impacting the ecosystems and the food chain [9]. CBA has been repurposed in the construction sector to address these concerns due to its sand-like texture and ability to be used as a coarse aggregate [10-12]. This alternative use of CBA offers several advantages, such as cost efficiency, lightweight properties, and its suitability as a substitute for natural quarried sand [13].

This study evaluates the potential of integrating CBA into polymer-based composites (PC) as a reinforcing component. Since CBA is rich in metal oxides, including silicon dioxide (SiO_2) and aluminium oxide (Al_2O_3), it functions effectively as a natural filler within polymer matrices. Research by Pappu [14] indicates that coal ash-reinforced polymeric composites exhibit superior strength to wood and plastic while offering durability, fire resistance, and cost-effectiveness. While extensive research has been conducted on CFA-based polymer composites, such as PANI/CFA [15], pyrrole/CFA [16], and epoxy/CFA [17] composites. According to Zainal et al. [18] and Akemal et al. [8], studies focusing on the incorporation of CBA in polymer composite systems remain limited due to its granular and porous structure, which affects the resulting polymer composite's properties. Thus, the modification of CBA during the pre-handling process is required to improve the compatibility between the reinforcement and matrix phases.

This research aims to develop a polypropylene-coal bottom ash (PP-CBA) composite. This research advances previous coal ash-based composite studies by shifting focus to CBA instead of CFA. The pre-handling process included sieving; an aspect that has not been extensively examined in prior PC research. Additionally, the study investigated the effects of heat treatment as a post-processing condition on the PP-CBA slab. These factors significantly influence the physical and mechanical properties of PP-CBA composites. As CBA is an industrial by-product, utilizing it as a raw material aligns with circular economic principles, promoting sustainability. The potential application of PP-CBA composites presents an opportunity to address environmental concerns while minimizing waste disposal challenges in the polymer industry.

2. MATERIALS AND METHODS

2.1 Pre-handling Conditions of CBA

The entire CBA collected from Manjung Power Plant, Perak Malaysia, was crushed, and part of the crushed CBA was sieved into a particle size of $\sim 250 \mu\text{m}$. The polypropylene composite exhibited the greatest strength when reinforced with coal bottom ash particles ranging from 250 to 300 microns in size [19].

2.2 Fabrication of PP-CBA Composite Pellets

For this study, 30% of the total composite composition was allocated to CBA-polymer composite. The CBA, both sieved and un-sieved, was blended with PP (Titanpro 6331) using a Muriyama Dispersion Mixer at a temperature slightly above the melting point of PP (190 °C). The mixing process continued until a uniform; putty-like consistency was achieved. The resulting blend was then extracted from the mixer and allowed to solidify at ambient temperature. Once hardened, the PP-CBA composite was crushed into smaller, uniform pellets, which were later utilized for slab fabrication

2.3 Fabrication of PP-CBA Composite Slabs

Each slab was fabricated by carefully placing a measured quantity of PP-CBA composite pellets into a pre-greased mold cavity (dimensions: 15 cm × 15 cm × 4 mm) to facilitate easy removal. The mold was then sealed with its cover and subjected to compression molding at 190 °C for 15 minutes under consistent pressure. Following this process, the mold was taken out and rapidly cooled at room temperature for 15 minutes in the cooling machine. Once cooled, the sample was detached from the mold.

The presence and influence of moisture content in the PP-CBA composite slabs, both before and after heat treatment, were investigated through a combination of FTIR spectroscopy, FESEM analysis, and mechanical impact testing. These techniques provided complementary evidence of moisture behavior throughout the fabrication and heat treatment processes. For the heat treatment analysis, the samples underwent additional drying in an oven at 50 °C and 100 °C for a duration of one hour. Slabs that were not heat-treated served as the control group.

2.4 Physical and Chemical Characterizations of Composites

To better understand the mechanical characteristics of the composite materials, all pallet and slab samples were analyzed using advanced instrumentation techniques. These analyses provided insights into key structural and physical attributes affecting their mechanical performance.

2.4.1 Field Emission Scanning Electron Microscope (FESEM)

The morphology of raw, un-sieved, and sieved CBA, along with their respective composites, was examined using a field emission scanning electron microscope (FESEM) SUPRA-40 VP. Since the composite specimens were non-conductive, they were pre-coated with a thin layer of gold using a BAL-TEC SCD 005 sputter coater before analysis under FESEM.

2.4.2 Fourier-Transform Infrared Spectroscopy (FTIR)

Fourier-transform infrared (FTIR) spectroscopy was conducted utilizing the Perkin Elmer Spectrum One Series, configured with a 4 cm⁻¹ resolution and scanned 16 times. This technique was applied to evaluate changes in the chemical structure of the composite system following modifications that influence the mechanical integrity of the slabs. The identification of key functional groups in each composite sample was recorded within the spectral range of 4000-450 cm⁻¹.

2.4.3 X-Ray Diffraction (XRD)

X-ray diffraction (XRD) analysis was conducted at room temperature using an XRD PANalytical X'Pert PRO diffractometer, with CuK α radiation ($\lambda = 1.5418 \text{ \AA}$). The diffraction patterns were recorded across a 2θ range of 10° to 90° at a scanning rate of 2.5°/2 θ per minute. These measurements were used to investigate phase transformations in the composites resulting from modifications that influence the mechanical properties of the slabs.

2.4.4 Drop Impact Test

The drop weight impact test was performed in accordance with ASTM D5628 guidelines, utilizing a Dynatup 8250 impact testing machine. The impact force was measured using a Kistler 9333A piezoelectric load cell positioned above the indenter. During testing, specimens (5 mm × 5 mm) were placed on two stainless steel cylindrical supports, each 12.5 mm in diameter. The drop tower was fitted with a 16 mm hemispherical impactor weighing 3.0 kg, which was released from a height of 75 mm to assess the material's impact resistance.

2.4.5 Physical Observation of Sieved and Un-Sieved Slabs

Surface images of the PP-CBA composite slabs were captured using a digital camera (iPhone 14 Pro Max) equipped with a 48 MP wide-angle lens. The slabs were placed on a matte-black background under natural lighting to reduce glare and enhance surface contrast. Photos were taken at a fixed distance of approximately 15 cm, with manual adjustments to focus and exposure settings. This setup allowed clear visualization of surface differences between sieved and un-sieved CBA samples.

3. RESULTS AND DISCUSSION

3.1 Effect of Pre-handling Conditions of CBA on the formation of PP-CBA Slabs

FESEM micrograph of the un-sieved raw CBA contains various un-crushed particle sizes scattered on the surface of the ash matrix (Figure 1 (a)). On the other hand, the sieved raw CBA (250 µm) exhibited smoother morphology than the un-sieved CBA (Figure 1(b)). This indicates that sieving was able to eliminate larger particles that may complicate the overall processing.

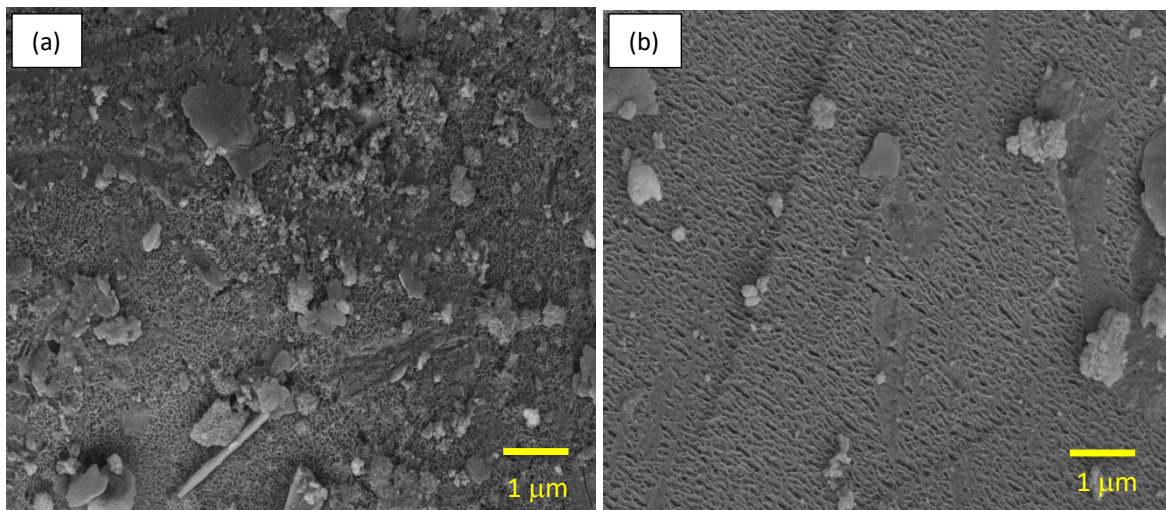


Figure 1: FESEM micrographs for raw (a) un-sieved and (b) sieved CBA

A more dented surface of the slab was obtained when un-sieved CBA was used in the fabrication of the slab (Figure 2(a)), compared to the smoother surface observed when sieved CBA was used (Figure 2(b)). This was probably due to the various particle sizes that were scattered on the surface, obstructing the flow of PP to mix with the CBA matrix homogeneously.

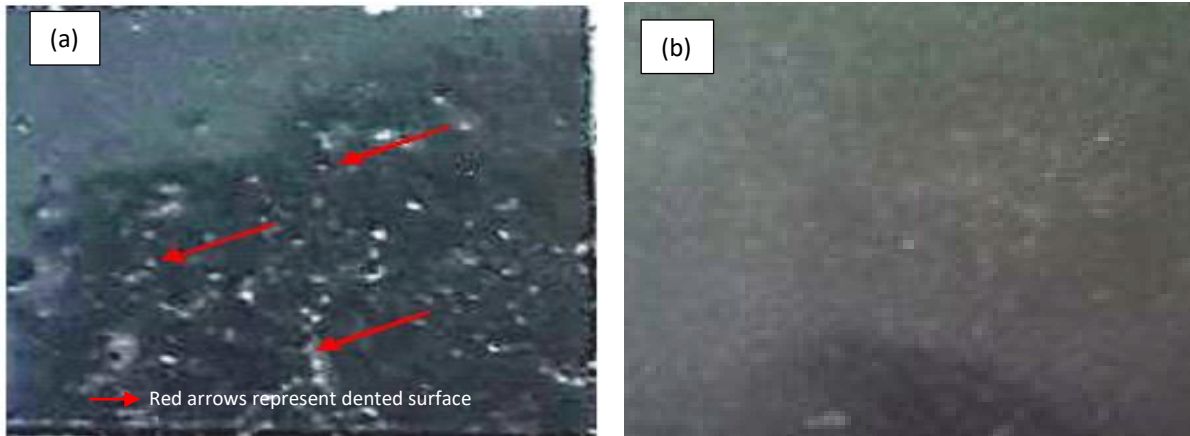


Figure 2: Photograph images of PP-CBA composite slabs consisting of (a) un-sieved and (b) Sieved CBA

The FESEM micrograph of the slab incorporating un-sieved BA (Figure 3(a)) exhibits a higher density of pores compared to the slab with sieved BA (Figure 3(b)). This indicates that the presence of larger, irregular particles in the un-sieved CBA disrupts the uniform flow of PP, limiting its ability to adequately fill the voids during processing.

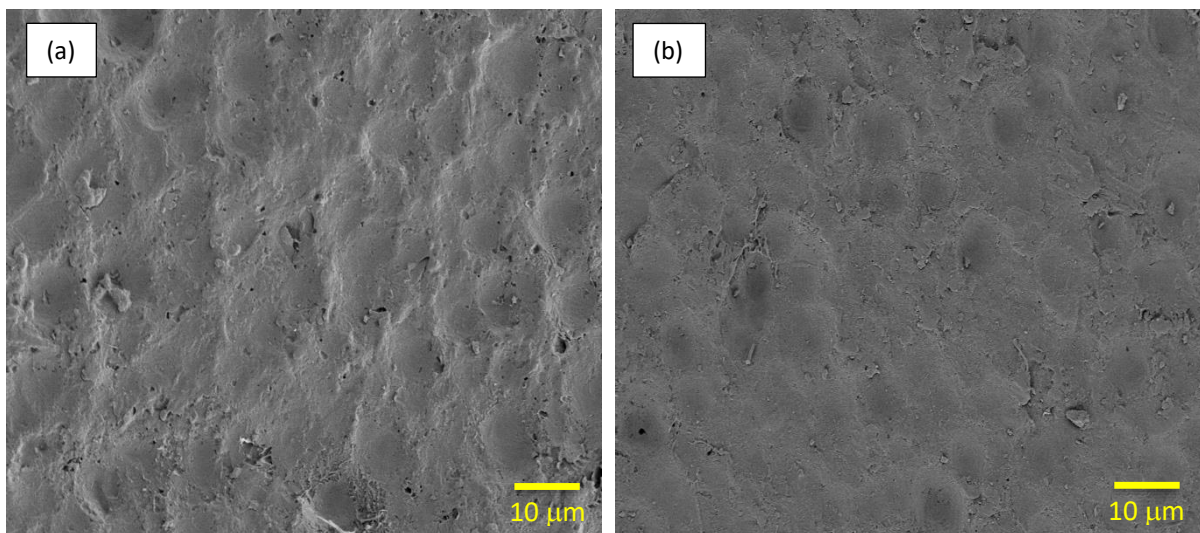


Figure 3: FESEM micrographs of PP-CBA composite slabs from (a) un-sieved and (b) sieved CBA

From the FTIR analyses, it was noted that extra handling of CBA like sieving causing it to expose to surrounding moisture (Figure 4). This can be confirmed from the presence of silanol group at $\sim 3300 \text{ cm}^{-1}$ [20] in the slab fabricated from the sieved CBA. This silanol group peak was not detected in the slab fabricated from the un-sieved BA.

In addition, due to the presence of high density of voids in the un-sieved PP-CBA composite, it was difficult for PP to orderly arrange during the fabricating process which be confirmed from its FTIR spectrum in which the isotactic peak of PP at $\sim 1160 \text{ cm}^{-1}$ [21] (Figure 5) was not detected. This indicates that this un-sieved PP-CBA composite exhibited less crystalline structure than the slab fabricated from sieved CBA and can be further confirmed by the reduction in the intensity of the 2θ peak of PP at 14° - 21° in its XRD diffractogram (Figure 6).

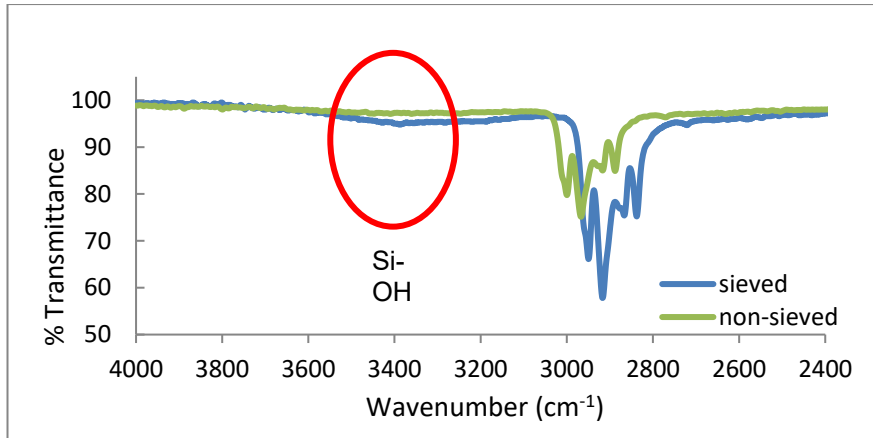


Figure 4: Si-OH Peaks in PP-CBA Composite Slabs from Un-sieved and Sieved CBA

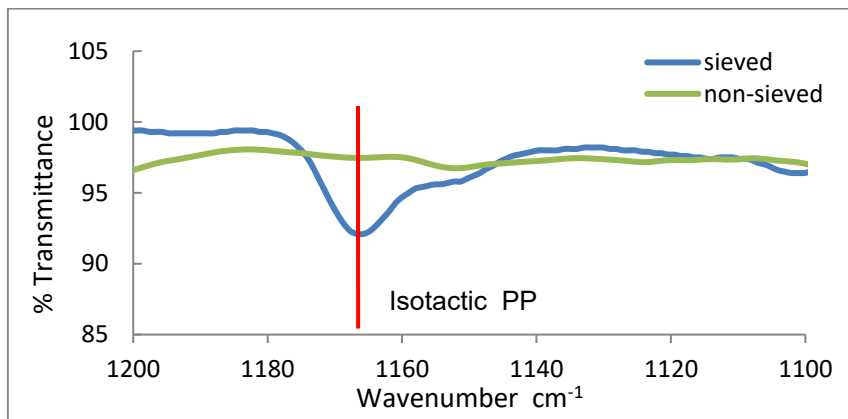


Figure 5: Isotactic Peaks of PP in PP-CBA Composite Slabs Un-sieved and Sieved CBA

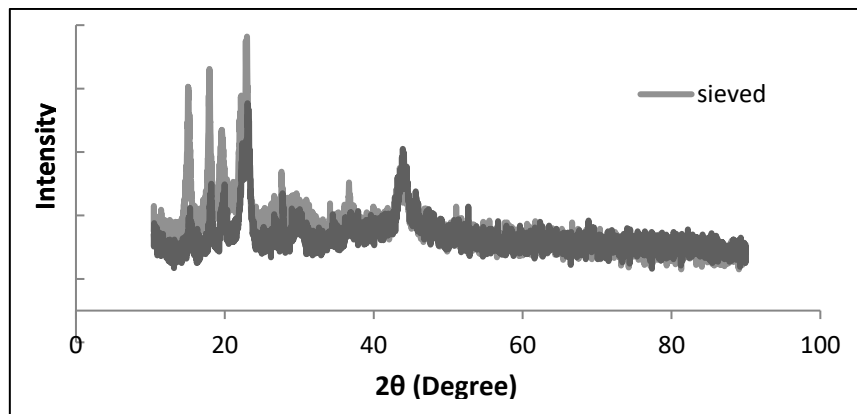


Figure 6: XRD diffractogram of PP-CBA composite slabs from un-sieved and sieved CB

It was found that this PP-CBA slab fabricated from the un-sieved CBA exhibited less impact strength (2.1 J) than its counterpart (3.4 J) due to the irregularity of filler shape and size and a more porous structure that limits the distribution of stress in the system. According to Beer et al. [22], stresses must be distributed uniformly throughout the material to achieve high impact strength, which explains why the PP-CBA from the un-sieved CBA specimen fractured after the drop impact test (Figure 7(a)). In contrast, the specimen fabricated with sieved CBA exhibited only localized cracking (Figure 7(b)),

a typical failure mode in porous materials where cracks initiate from existing pores, acting as propagation sites.

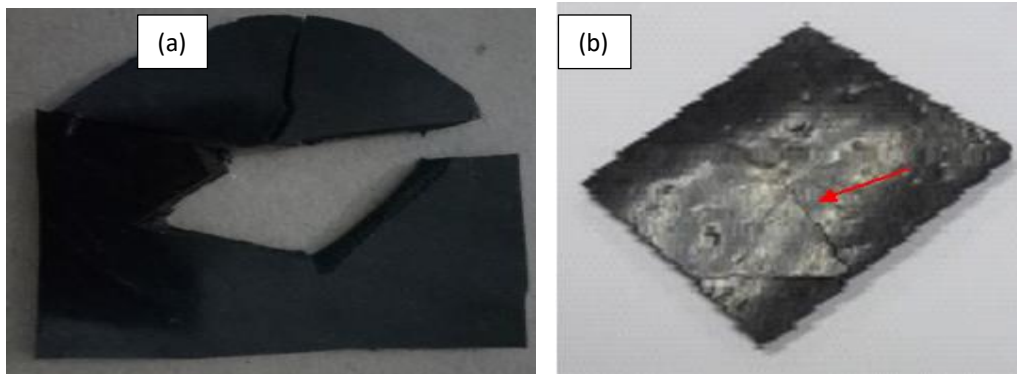


Figure 7: Photograph images of PP-CBA composite slab specimens from (a) un-sieved and (b) sieved CBA after drop impact test

Therefore, it can be concluded that sieving the CBA before the fabrication of the slab is important to obtain uniform particle size to control the flow of the PP into the porous CBA matrix during the mixing. For the following heat treatment studies, all the CBA was sieved to a specific size of 250 μ m prior to the fabricating process.

3.2 Effect of Heat Treatment Temperatures on PP-CBA Slabs

The heat-treated slabs exhibited a more dented surface morphology, likely caused by the escape of moisture interacting with silica at the slab surface, as seen in Figure 8(b–c). In contrast, the untreated slab (Figure 8(a)) showed a relatively smoother surface, while surface denting became more pronounced with increasing treatment temperatures (50 $^{\circ}$ C and 100 $^{\circ}$ C). Additionally, porous structures were observed along the side edges of the heat-treated specimens (Figure 9).

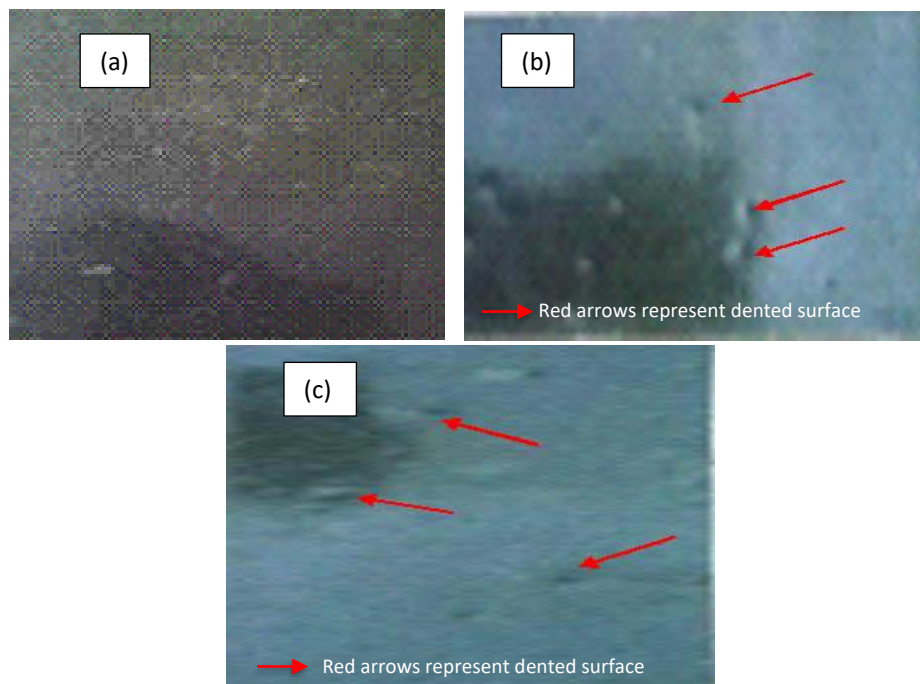


Figure 8: Photograph images of PP-CBA composite slabs at different heat treatments: (a) untreated, (b) treated at 50 $^{\circ}$ C and (c) treated at 100 $^{\circ}$ C

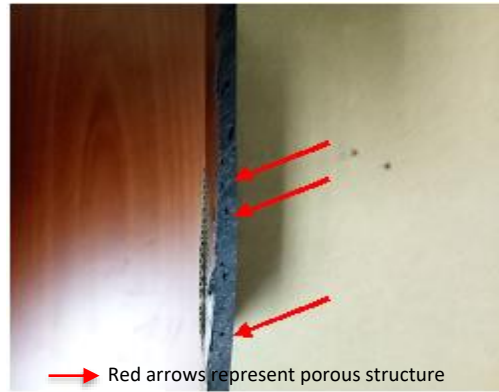


Figure 9: Photograph images of porous structures from the side edges of the heat-treated slabs

As shown in the FESEM micrographs (Figure 10(a)–(c)), minimal surface changes were observed in the untreated and 50 °C-treated slabs (Figure 10(a) and 10(b)), while noticeable ejection of particles occurred in the slab treated at 100 °C (Figure 10(c)). This suggests that at higher temperatures, volatile components such as moisture were able to escape from the composite system. A similar observation was reported for slabs subjected to high-pressure conditions during fabrication [23].

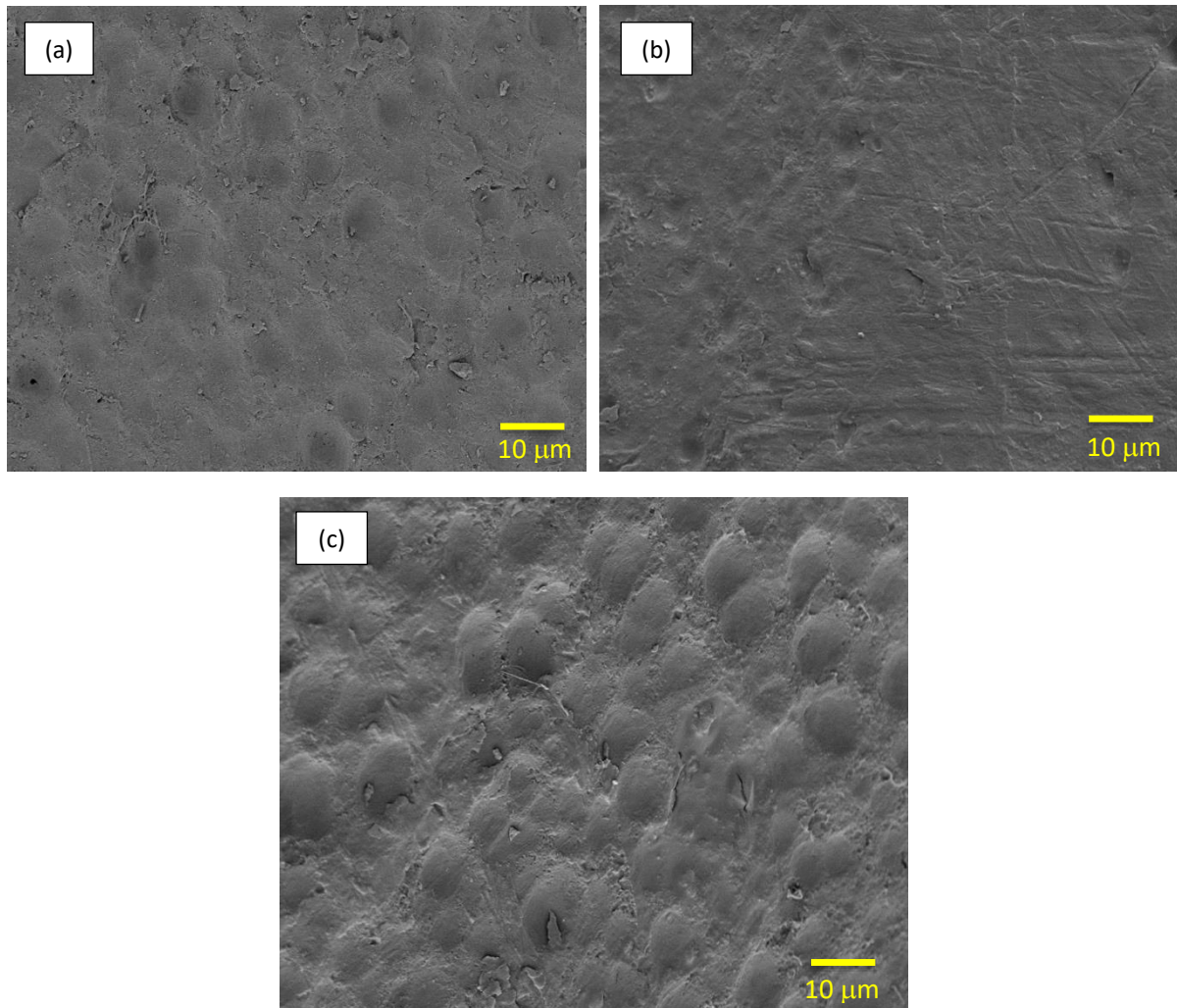


Figure 10: FESEM micrographs for PP-CBA composite slabs at different heat treatments (a) untreated, (b) treated at 50 °C and (c) treated at 100 °C

It was noted that after the heat treatment, the Si-OH peak at $\sim 3300\text{ cm}^{-1}$ was almost diminishing (Figure 11(a)) hence confirms that the moisture content had been released from the surface of the slabs. This explains why a more dented surface of the treated slabs was obtained. As a result, these additional voids became hindrance for the PP to orderly arrange and form less crystalline structure of the PP-CBA composites. This can be confirmed from the reduction of the isotactic peak of PP at $\sim 1160\text{ cm}^{-1}$ (Figure 11(b)) and the reduction of its XRD crystalline peaks (Figure 12). However, the phase change was not significant.

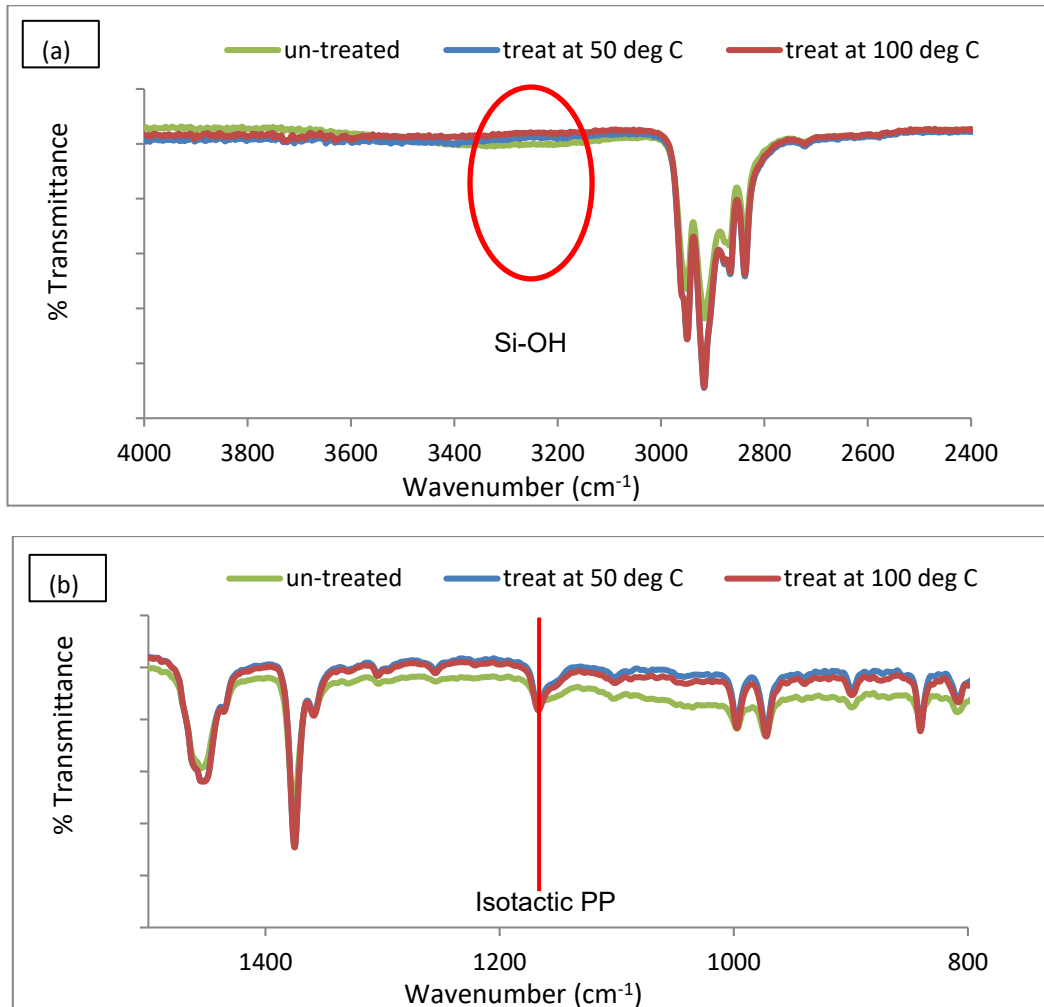


Figure 11: (a) Si-OH and (b) isotactic peaks for PP-CBA composites at various heat treatments

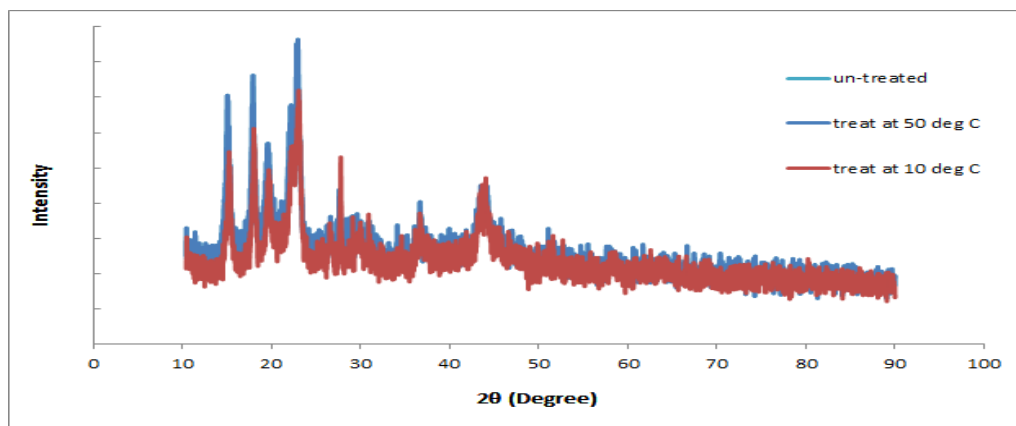


Figure 12: XRD diffractogram for PP-CBA slabs at various heat treatments

Figures 13 and 14 illustrate the impact of heat treatment on the mechanical performance of PP-CBA composite slabs. As shown in Figure 13, the impact energy dropped sharply from 3.3 J (untreated) to 1.6 J at 50 °C, with a slight recovery to 1.9 J at 100 °C, indicating reduced impact resistance with heat. Figure 14 visually confirms this trend: the untreated slab (a) remains mostly intact, while heat-treated slabs at 50 °C (b) and 100 °C (c) show significant failure, with visible punctures. The relationship between these two figures illustrates that the loss in impact energy is directly associated with the visible mechanical degradation of the slabs. This degradation is attributed to the disruption of polymer chain arrangement and reduced crystallinity caused by heating. Additionally, in a hygroscopic system containing CBA, the presence of Si-OH groups may also influence the mechanical strength. Hence, these findings collectively highlight the negative impact of thermal treatment on the structural and mechanical integrity of PP-CBA composites.

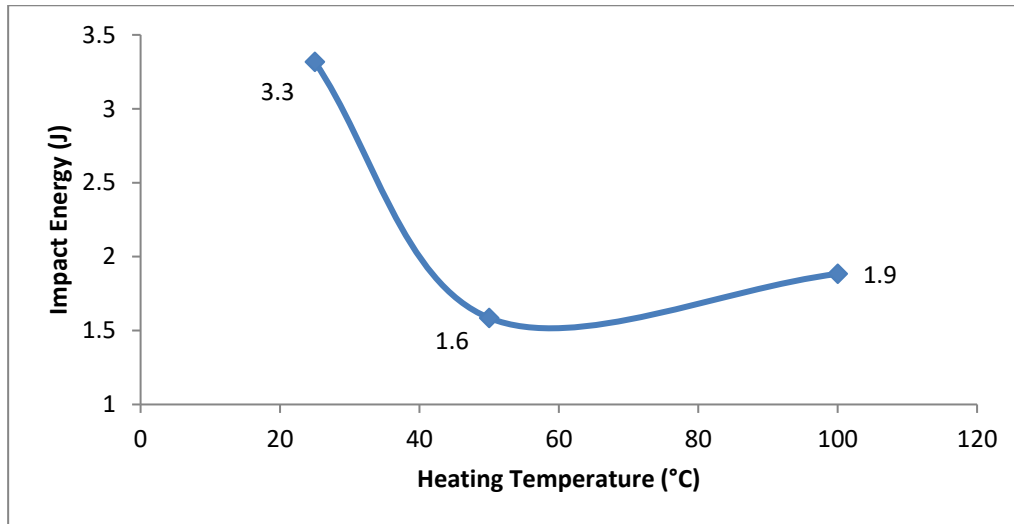


Figure 13: Average drop impact energy for PP- CBA composite slabs at various heat treatments

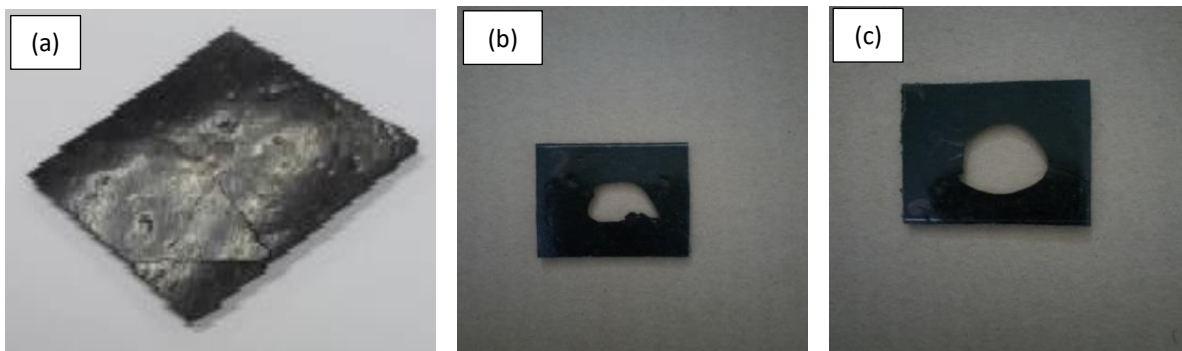


Figure 14: Photograph images of drop impact specimens for PP-CBA composite slabs at different heat treatments: (a) untreated, (b) treated at 50 °C and (c) treated at 100 °C.

4. CONCLUSIONS

It can be concluded that CBA is a potential filler for developing a green polymer composite system. However, special handling, such as sieving, is required to obtain uniform particle size in order to control the flow of the PP into the porous CBA matrix during the mixing. Interestingly, the slabs required no further heat treatment since the presence of moisture that attaches to the silica group of CBA imparts a certain degree of mechanical strength. PP-CBA composites offer a sustainable and cost-effective solution for construction (cable protection slabs, structural panels), automotive (dashboard

components, battery casings), packaging (lightweight pallets, recyclable containers), infrastructure (road signage, barriers), and furniture (decorative panels, molded chairs) due to their balance of mechanical strength, durability, and environmental benefits. Studies on the PP-CBA composites' mechanical and thermal stability under a broader range of temperatures, long-term ageing and environmental exposure are necessary to provide a more comprehensive assessment of their durability and reliability in real-world applications. Furthermore, alternative processing methods can be explored by optimizing filler-matrix compatibility through the investigation of various surface treatments and compatibilizers to enhance adhesion and improve the mechanical performance of the composite.

Acknowledgments

The authors gratefully acknowledge the financial support provided by TNB Research Sdn. Bhd. through its internal fund. The authors also extend their sincere appreciation to the Faculty of Applied Sciences, Universiti Teknologi MARA (UiTM) Shah Alam, for granting access to research equipment and laboratory facilities essential to the completion of this project.

Author Contributions

All authors contributed towards data analysis, drafting and critically revising the paper and agree to be accountable for all aspects of the work.

Disclosure of Conflict of Interest

The authors have no disclosure to declare.

Compliance with Ethical Standards

The work is compliant with ethical standards.

References

- [1] Rashidi, N. A., Chai, Y. H. & Yusup, S. (2022). Biomass energy in Malaysia: current scenario, policies, and implementation challenges. *Bioenergy research*, 15(3), 1371-1386.
- [2] Benavidez, E., Grasselli, C. & Quaranta, N. (2003). Densification of ashes from a thermal power plant. *Ceramics International*, 29(1), 61-68.
- [3] Ali, R., Daut, I. & Taib, S. (2012). A review on existing and future energy sources for electrical power generation in Malaysia. *Renewable and Sustainable Energy Reviews*, 16(6), 4047-4055.
- [4] Beddu, S., Basri, N. A. N., Kamal, N. L. M., Mohamad, D., Itam, Z., Sivakumar, N. & Nazri, F. M. (2024). Characterization of coal combustion products from Malaysian power plant for building materials applications. *MATEC Web of Conferences*, 400, 01007.
- [5] Dung, T. T. T., Vassilieva, E., Swennen, R. & Cappuyns, V. (2018). Release of trace elements from bottom ash from hazardous waste incinerators. *Recycling*, 3(3), 36-54.
- [6] Parvin, F. & Tareq, S. M. (2021). Impact of landfill leachate contamination on surface and groundwater of Bangladesh: a systematic review and possible public health risks assessment. *Applied water science*, 11(6), 100-117.

- [7] Ganesan, H., Sachdeva, A., Petrounias, P., Lampropoulou, P., Sharma, P. K. & Kumar, A. (2023). Impact of fine slag aggregates on the final durability of coal bottom ash to produce sustainable concrete. *Sustainability*, 15(7), 6076.
- [8] Akemal, M. N., Kamal, M. M. F., Famiza, A. L., Asiah, M. N., Fadli, M. S., Fetri, Z. M. & Natasha, M. N. (2023). Non-conforming fibre-reinforced green polypropylene composite panels: a case study. *Journal of Material Cycles and Waste Management*, 25(4), 2025-2036.
- [9] Hauashdh, A., Mohamed, R. M. S. R., Nagapan, S., Abd Rahman, J. & Gamil, Y. (2024). Assessment of the environmental impacts of utilizing coal ashes and OPC for soil stabilization applications: Leachate analysis in response to rainfall interaction. *Case Studies in Construction Materials*, 21, e03672.
- [10] Lovrenčić Butković, L., Mihić, M., Nahod, M. M. & Sigmund, Z. (2022). The benefits of cost-benefit analysis in construction projects. *15th International Conference Organization, Technology; 6th International Project Management Association Senet Conference*, 532-545.
- [11] Opon, J. & Henry, M. (2019). An indicator framework for quantifying the sustainability of concrete materials from the perspectives of global sustainable development. *Journal of Cleaner Production*, 218, 718-737.
- [12] Miraldo, S., Lopes, S., Pacheco-Torgal, F. & Lopes, A. (2021). Advantages and shortcomings of the utilization of recycled wastes as aggregates in structural concretes. *Construction and building materials*, 298, 123729.
- [13] Ghadzali, N. S., Ibrahim, M. H. W., Zuki, S. S. M., Sani, M. S. H. & Al-Fasih, M. Y. M. (2020). Material characterization and optimum usage of coal bottom Ash (CBA) as sand replacement in concrete. *International Journal of Integrated Engineering*, 12(9), 9–17.
- [14] Pappu, A. (2015). Recent advances on coal ash particulates' fortified glossy finish polymer composites. In proceedings of the *World of Coal Ash*, World of Coal Ash (WOCA) Conference in Nashville, TN, May 5-7, 2015.
- [15] Umejuru, E. C., Prabakaran, E. & Pillay, K. (2023). Coal fly ash decorated with graphene and polyaniline nanocomposites for effective adsorption of hexavalent chromium and its reuse for photocatalysis. *ACS Omega*, 8(20), 17523–17537.
- [16] Yang, S., Liu, X., Zhang, Y., Chen, J. & Zhou, C. (2023). Effect of the coal fly ash blending ratio on biomass slagging structure modification and alkali metal migration. *Energy & Fuels*, 37(16), 12018–12029.
- [17] Sim, J., Kang, Y., Kim, B. J., Park, Y. H. & Lee, Y. C. (2020). Preparation of fly ash/epoxy composites and its effects on mechanical properties. *Polymers*, 12(1), 79.
- [18] Zainal, M. F., Yapandi, M. F. K., M Ahmad, S. A (2020). The effect of coal bottom ash in mechanical & environment performances for construction materials. *IOP Conference Series: Earth and Environmental Science*, 476(1), 012028.
- [19] Al Biajawi, M. I., Embong, R., Muthusamy, K., Ismail, N. & Obiany, I. I. (2022). Recycled coal bottom ash as sustainable materials for cement replacement in cementitious Composites: A review. *Construction and Building Materials*, 338, 127624.
- [20] Kalaw, M. E., Culaba, A., Hinode, H., Kurniawan, W., Gallardo, S. & Promentilla, M. A. (2016). Optimizing and characterizing geopolymers from ternary blend of Philippine coal fly ash, coal bottom ash and rice hull ash. *Materials*, 9(7), 580.

- [21] Prabowo, I., Pratama, J. N. & Chalid, M. (2017). The effect of modified ijuk fibers to crystallinity of polypropylene composite. *IOP Conference Series: Materials Science and Engineering*, 223(1), 012020.
- [22] Beer, F. P. & Johnston, E. R. (2006). *Mechanics of Materials*. 5th edition (McGraw Hill) pp. 693-696.
- [23] Grunenfelder, L. K. & Nutt, S. R. (2010). Void formation in composite prepregs - Effect of dissolved moisture. *Composites Science and Technology*, 70(16), 2304–2309.